SSRG International Journal of Electrical and Electronics Engineering
ISSN: 2348-8379/ https://doi.org/10.14445/23488379/IJEEE-V13I3P111

Volume 13 Issue 3, 140-151, March 2026

Original Article

Energy-Efficient EV Battery Charging using Dual Active Bridge Converter and Binary Chaotic Catch Fish Optimization

M.J. Murali[1] , S. Lakshmi[2]

[1,2]*Department of Electrical and Electronics Engineering, Bharath Institute of Science and Technology, Bharath Institute of Higher Education and Research, Selaiyur, Chennai, Tamilnadu, India.*

[1]*Corresponding Author : muralimj2019@gmail.com*

Received: 09 December 2025 Revised: 11 January 2026 Accepted: 16 February 2026 Published: 31 March 2026

Abstract *- EV Battery charging with dual functionality in energy efficiency. An Electric Vehicle (EV) battery recharging system built based on an optimized Dual Active Bridge (DAB) DC-DC converter, which can operate in both Constant Current (CC) and Constant Voltage (CV) modes. The DAB converter is ideal in all EV applications in the modern day because it features Zero Voltage Switching (ZVS), bidirectional power flow, and galvanic isolation with a High-Frequency Transformer (HFT). CV mode uses Dual Phase Shift (DPS) modulation, whereas CC mode uses Extended Phase Shift (EPS) modulation. A Proportional-Integral-Derivative (PID) controller regulates the CV charging process, whereby the gains are optimally set through the Binary Chaotic Catch Fish Optimization Algorithm (BCCFOA). To ensure rapid and constant dynamic response, the tuning is formulated on the minimization of the Integral of Time-Weighted Absolute Error (ITAE). The comparative analysis reveals that the lowest standard deviation of 2.08 X 10-3 is reached at BCCFOA, which is better than CFOA, TSA, and PSO algorithms. An LCL filter is added to reduce the harmonics and improve the quality of power. The findings of the simulation in MATLAB/Simulink show that the peak overshoot has been reduced by 5 percent, the settling time is 1.0 s, and the minimum rise time is 0.28 s with the PID and LCL. The accuracy and consistency of charging is proven by the State of Charge (SoC) curve, which rises smoothly with an increase of 54.95% in 1 second. These findings confirm that the system proposed is effective regarding the provision of optimized, stable, and high-quality EV battery charging performance.*

Keywords *- Binary chaotic catch fish optimization, Dual active bridge converter, High-frequency transformer, LCL filter, PID controller.*

1. Introduction

The growing necessity to decarbonize the transportation industry has jump-started the swift growth in the use of Electric Vehicles (EVs) globally. This expansion indicates a firm consumer switch from internal combustion engines to electric motors. Nevertheless, there are also two significant bottlenecks to the widespread implementation of EVs: range anxiety and long charge times. Most traditional EV chargers incorporate AC-DC converters, which are linked to the AC grid. However, DC-DC converters are becoming increasingly popular as DC microgrids and renewable energy systems are becoming increasingly popular. These converters allow more compact and scalable charger designs, reduce losses in energy, and eliminate unnecessary power conversion stages. Because of their ability to offer galvanic isolation, bidirectional power flow, and voltage equality, Isolated Bidirectional DC-DC (IBDC) converters are now a possible alternative in this aspect as well. The DAB converter has received the highest interest in the array of IBDC topologies used in charging EV batteries. Its soft-switching, modular scalability, and support of various phase-shift-based modulation schemes make it suitable for either Vehicle-to-Grid (V2G) or Grid-to-Vehicle (G2V) applications [1]. There are many modulation procedures proposed to improve the functioning of DAB converters in the application of electric vehicles. The basic form of the DAB converter to charge the battery is presented in Figure 1. Even though the Single-Phase Shift (SPS) method is easy and very common, there are disadvantages to it in terms of dealing with large changes in voltages and the variety of load conditions. In response to the need for a wide voltage regulation, Rafi et al. [2] developed a semi-dual active bridge converter based on a real-time phase shift control method. This technique is often used in EV charging stations that include an Energy Storage System (ESS), which varies the gain dynamically between changing input and output voltage levels. With the rising number of EVs, the facility to charge them needs to be capable of servicing more than one vehicle simultaneously. Nazih et al. [3] propose a multiport DAB topology, which is Ring-

Connected DAB (RCDAB), that allows flexibility in internal routing of power and dynamic port usage. Their method reduces RMS current and unwanted power processing through a bisection-based optimization strategy. In order to optimize the converter efficiency, more sophisticated modulation methods have been investigated in addition to topological ones. Jiang et al. [4] tested the Triple Phase Shift (TPS) control modes of DABs. They could determine trade-offs and the best configurations with various operating conditions because they could evaluate and adjust various objectives, such as power backflow, RMS current, and ZVS.

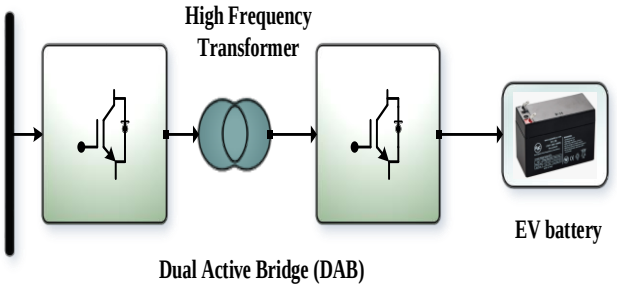

Fig. 1 Conventional DAB converter model for battery charging

Chen et al. [5] further included a hybrid DAB utilizing two transformers to enhance the efficiency even higher with the high voltage loads. The leg and transformer of the normal DAB were divided into halves, and this greatly enhanced the flexibility of control. Barresi et al. [6] proposed the unified-segmental control system that minimized integration of the grid infrastructure to Modular Multilevel Converters (MMC) and DAB converters by reducing switching losses and inrush currents. Huge transformers and filters are not needed since the proposed approach would be linked directly to the Medium Voltage (MV) grid. A process of parameter selection in DAB maximizes the soft-switching zones and ensures maximization of internal balancing as per the power cycle simulation.

The potential of DAB converters is fully loaded with such issues as weak ZVS when operating under light load conditions, inefficient charging over wide voltage ranges, and stability issues in DC microgrids, as EVs gain in popularity. In the case of dynamic operating conditions, the traditional methods of control, SPS and DPS, often lead to high reactive power and current stress.

Multiport DAB networks also make fault tolerance and control of power flow even more difficult, despite their possible ability to provide a scalable, fast-charging infrastructure. Due to these disadvantages, advanced designs of DAB converters with adaptive control schemes, high efficiency, improved soft-switching features, and consistent integration with modern EV charging structures are needed. The main contributions that the research work makes are as follows:

- To charge an EV battery, the DAB DC-DC converter employs the modulation techniques of EPS and DPS to support the CC and CV states.
- The algorithm used is the BCCFOA, which is employed to enhance the settings of the PID controller of CV mode regulation, leading to better stability and dynamic response.
- To achieve improved quality of power and grid compliance, an LCL filter is applied at the output stage to effectively minimize the high-frequency switching harmonics. The effectiveness, rapid convergence, and generality of the proposed control scheme for real-time EV charging use are validated by the results of the entire DAB-based EV charging system that can be simulated and analyzed in the simulation environment.

2. Literature Survey

Recent advances in DAB converters show their suitability in the rapid, efficient, and two-way transmission of power through the EV charging systems. A power management control strategy proposed by Ri es et al. [7] to freestanding DC microgrids in which DABs were implemented to couple Battery Energy Storage Systems (BESS) to Renewable Energy Sources (RES). Their nonlinear resilient control enhanced the dynamic power stability and power allocation during dynamic power loads and stable power loads. In the meantime, additional research is undertaken with respect to DAB topologies that are being modified to suit an expanded range of application requirements. These improvements in a detailed assessment are put together as modular units like active bridges, transformers, and supplemental networks [8].

The framework is used as a guide in an attempt to design customized DAB topologies that are specific to either power, voltage, or control constraints. The complexity of control is raising the requirements of more intelligent modulation. Phase varying is dynamically adjusted in this technique to minimize reactive power and enhance the ZVS region, particularly with weak loads. Experiment and simulation on a 2kW prototype revealed a better efficiency and stable operation. Intermediate between AC and DC systems, [10] proposed a Semi-Dual-Active-Bridge (SDAB) AC/DC converter that is able to achieve Power Factor Correction (PFC), as well as soft switching, in a single-stage architecture. The converter is compact and highly efficient by removing the bulky intermediate capacitors and utilizing continuous/discontinuous current mode, which has been experimentally proven.

Nallamothu et al. [11] made comparisons between PI and Fuzzy Logic Controllers (FLC) when using solar-integrated DAB systems; they found that FLCs cope with the dynamism in solar irradiance and battery load in comparison to the traditional PI controllers. In a study to overcome drawbacks of efficiency in the traditional five-level DAB topology, Haq et

al. [12] came up with a simplified design, using fewer elements, and adopted Particle Swarm Optimization (PSO)-based modulation to enhance performance. In order to provide further control, hybrid metaheuristic algorithms such as artificial ecosystem-based optimization and manta-ray foraging optimization algorithm AEO-CMRFO [13] and PSO-DMC (Dynamic Matrix Control) [15] have been used to control the optimization of fractional-order controllers and reduce current stress under extended-phase-shift control. Moreover, Graphical Optimization (GSO) techniques [14] provide easy and efficient means to increase DAB performance without complicated calculations.

Many papers research the problem of complex PID controller tuning with respect to DC-DC converters, and methods based on nature. An example is the Firefly [16], Golden Eagle Optimization (GEO) [17], and Gray Wolf Optimization (GWO) [18] settings of PID that have enhanced dynamic responses, reduced voltage swings, and reduced settling times. Such strategies are used in more complicated systems, such as offshore wind energy systems [20] and switching reluctance motors [19], in which optimization-based FOPID controllers have been shown to be more dependable and efficient. These efforts combined demonstrate the importance of smart control and optimization approaches to the increased efficiency, functionality, and scalability of DAB-based power conversion systems.

All these operations prove the necessity of clever control and optimization methods in increasing the performance, flexibility, and scale of power conversion based on DAB. Also, the inability of the conventional PID controllers to adjust to nonlinear dynamics and evolving load conditions lowers the stability and efficiency of the entire system. These limitations are exacerbated by the fact that fault-tolerant power flow management, as well as real-time load balancing, must be realized in complex multiport DAB systems. Therefore, demand a superior control system that employs metaheuristic optimization methods like Particle Swarm Optimization (PSO), GWO, or hybrid solutions to optimize switching schemes and controller parameters. This optimization may minimize power losses, offer much more flexibility in the system, and provide reliable operation in dynamic EV charging environments.

3. Proposed Methodology

To charge EV batteries, a DAB DC-DC converter that incorporates integrated ZVS, bi-directional power transfer, and galvanic isolation is developed to execute the conversion by linking two active H-bridges with a High Frequency Transformer (HFT). These features make the DAB converter a good fit for EV charging operations. This paper examines the design and operation of the DAB converter when in the CC and CV charge modes. Binary Chaotic Catch Fish Optimization Algorithm (BCCFOA) helps to improve the performance of a PID controller operating in the CV mode by optimization of its settings. It also has an LCL filter in order to enhance power quality and reduce harmonics.

The proposed DAB-based EV charging system is simulated and modeled in the simulation environment to prove the effectiveness of the method. The results are then discussed. Figure 2 expounds on the flow of the proposed methodology.

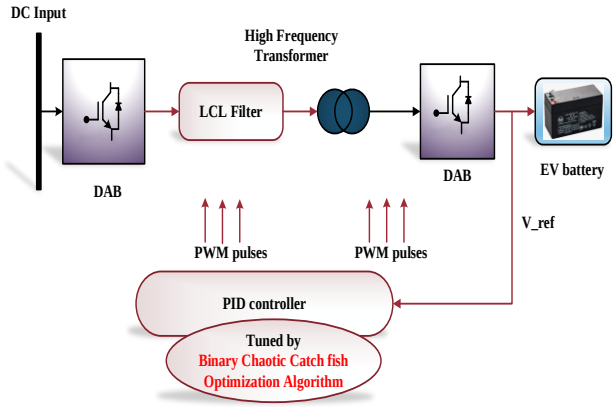

Fig. 2 Block diagram of DAB DC-DC converter-based BCCFOA methodology

3.1. DAB DC-DC Converter

DAB topology allows power to flow in both directions, and ZVS is inherent, thus making it a good choice. DAB is based on the concept of power transmission of the power systems on the basis of AC power. The direction of power in a pair of points in a power system is controlled by the phase difference between the voltages of two points. The EV battery charging system design has a DAB converter that is between the EV batteries [21]. The HFT connects the two active full bridges on the input/output of the DAB converter. Primary bridge input is linked to four IGBT switches, namely S1, S2, S3, and S4, and the output is linked to IGBT switches M1, M2, M3, and M4 that form the secondary bridge. This is then followed by the secondary bridge. The switches of main S1 and S4 or S2 and S3 are done simultaneously, and the switches connected to the same leg (S1, S3, or S2, S4) in a complementary manner. The high-frequency square wave Voltages (Vp and Vs), which are the main and auxiliary ones, indicate the differences in phase between the Voltage Across The Inductor (VL). The magnitude and direction of power flow can be changed by setting the phase shift (ϕ) between the voltages of the individual active bridges. The power transmission between the DAB converter can be determined by using one.

$$P_{Conv}=\frac{nV_PV_S}{2\pi^2fL}\phi(\pi-\phi) \quad (1)$$

Here, the turns ratio is denoted as n, and f represents switching frequency.

According to the traditional converters, LCL filter-based DAB converters have an LCL resonant tank instead of a single filter inductor. Based on the topology schematic Figure 3, the resonant tank consists of two filter inductors L1 and L2 and a filter capacitor C1.

The leakage inductor of the transformer is converted to a filter inductor L2 on the primary side. In a symmetric configuration, the HFT ratio is 1: N, and L1 and L2 are considered equal in the analysis below. Figure 4 shows the model of the suggested converter that is LCL-based. The suggested converter is a two-port circuit, which is derived from a similar model as shown in Figure 4, where Equation (1) is the representation of the input and the output characteristics. The resonant frequency is written as "s1) (1)/ sqrt (L C 1) and resonant impedance is written as Z 0) = s1) L= sqrt (L/ C 1). In this case, L is the sum of the inductance of the filter inductors "L" _"1" and "L" _"2" 2. When the switching frequency equals "ω", then resonance takes place.

$$\begin{cases} \dot{U}_P = j\left(\omega L_1 - \frac{1}{\omega C_1}\right)\dot{I}_P + j\frac{1}{\omega C_1}\dot{I}_S \\ \dot{U}_S = j\left(\frac{1}{\omega C_1} - \omega L_2\right)\dot{I}_S - j\frac{1}{\omega C_1}\dot{I}_P \end{cases} \quad (2)$$

$$\begin{cases} \dot{U}_P = jZ_0\dot{I}_S \\ \dot{U}_S = jZ_0\dot{I}_P \end{cases} \quad (3)$$

From Equation (2), it is observed that $\dot{U}_P$ leads $\dot{I}_S$ by 90∘, while $\dot{I}_P$ leads $\dot{U}_S$ by 90◦. When $\dot{U}_S$ is shifted by 90◦relative to $\dot{U}_P$The voltage and current on both sides become in phase, indicating the absence of reactive power.

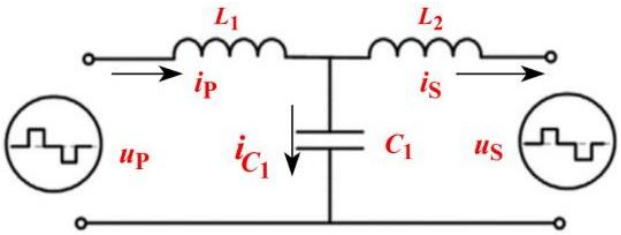

Fig. 3 LCL filter

The DAB converter has four intervals of the conduction states depending on the switching patterns of the Primary (S) and Secondary (M) side switches. During the first half-cycle (t 0-t 1), switches S 1, S 4, and M 1, M 4 turn on, allowing the flow of power in the primary to secondary through a positive current. During the second period (t 1 t2), S 1, S 4 remain conductors with the secondary switches switching to M 2, M 3 and power being transferred through the secondary circulating current, reversing its direction.

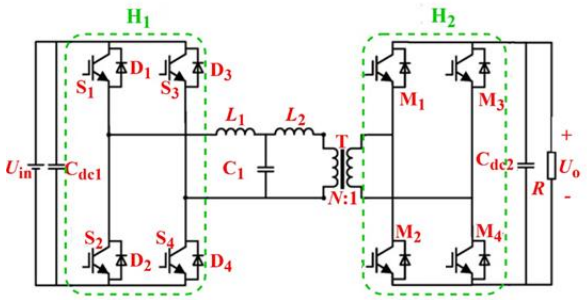

Fig. 4 LCL filter connected to the DAB converter

In the third interval (t 2 t 3), support S 2 S 3 and M 2 M 3, and both sides of the power flow in the negative current occur. Lastly, in interval four (t 3-t 4), S 2, S 3 will be active with the secondary switches returning to M 1, M 4, and the reverse power transfer will occur once more as the current on the secondary side is reversed again. The conduction of the proposed converter is presented in Table 1.

3.2. PID Controller for DAB Converter

The modulation method that is extensively deployed in DAB converters is the PID controller. The phase shift ratio, D=ϕ/pi where ϕ is the angle of phase shift between the voltages of the primary and secondary bridges, is used to control the power circulated in such converters. The ratio is directly proportional to the transmitting power. In the case of a DAB converter, the altered power transfer equation with D is formulated in the form of the Equation of the type of (4),

$$P_{Conv} = \frac{nV_PV_S}{2\pi^2 fL} D(1-D) \quad (4)$$

This Equation demonstrates that the power flow control in the DAB is achieved by the ratio of phase shift, which is denoted by D, which has a direct relation to the level of transferred energy in every switching period. The suboptimization of the PID controller makes it possible to regulate the "D" with greater accuracy, which guarantees the stability of power conversion and its efficiency.

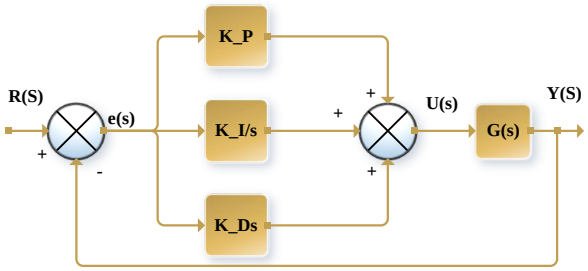

Fig. 5 Block diagram of PID controller

A PID controller is a type of system feedback that is used to assess and improve the precision of an instrumentation system. They are popular, for example, for improving the

dynamic response and reducing steady-state errors. The transient response is enhanced by the derivative element, and the steady-state inaccuracy is eliminated by the integral part. Figure 5 shows the three fundamental components of the controller: Proportional (P), Integral (I), and Derivative (D). These components may be used separately or together, depending on the nature of the system (plant) and the performance required. The mathematical model of the PID controller is in Equations (5) and (6).

$$k_P+\frac{k_I}{s}+k_d s=\frac{k_D s^2+k_P s+k_I}{s} \quad (5)$$

$$k_P+k_i\int e dt+k_D\frac{de}{dt} \quad (6)$$

The operating principle of the PID controller states that the control signal is applied to the plant in order to get the desired output. The output obtained is then passed back to the sensor, where the new error is computed by comparing the output with the reference value.

The PID controller utilizes this new error to calculate the correct control action by modifying the gain values “k” _“P”,” “K” _“I”, and “K” _“D” to keep on refining the system response to achieve the best performance possible.

Table 1. Conduction states of the DAB converter with remarks

Interval	Time Duration	Conducting (Primary)	Conducting (Secondary)	Observations
1	t_0-1_1	S_1, S_4	M_1, M_4	Power flows from primary to secondary; positive current.
2	t_1-t_2	S_1, S_4	M_2, M_3	Power transfer continues; current reverses in the secondary.
3	t_2-t_3	S_2, S_3	M_2, M_3	Power flows from secondary to primary; negative current.
4	t_3-t_4	S_2, S_3	M_1, M_4	Power transfer continues; current reverses in the secondary.

3.3. Binary Chaotic Catchfish Optimization Algorithm

The Catch Fish Optimization Algorithm (CFOA) [22] is a nature-inspired metaheuristic algorithm, which is founded on the group dynamics of fish preys capturing prey in the water. It emulates the dynamic and adaptive search and exploitation behavior of fish to search and explore the search space and optimize it globally. The movement is coordinated by a sense of vibrations, light, and water currents, and the pathways of fish are adjusted dynamically to maximize the likelihood of a prey being caught. Fish locate food/prey depending on the cues in the local environment and relocate to promising areas. It is true that some fish are leaders, and others are followers, by updating their positions in the best solutions discovered. This algorithm weighs the broad search (exploration) and refinement (exploitation) with the help of dynamic position updating.

Binary Chaotic Catch Fish Optimization Algorithm (BCCFOA) is an improvement of the CFOA, which incorporates binary encoding to solve discrete optimization problems such as PID controller tuning. It also uses chaotic maps, e.g., logistic maps, to increase diversity in a population and avoid early convergence. Also, in EV battery systems to optimally tune the PID parameters in DAB converters, BCCFOA is successfully applied.

It reduces control errors on the basis of criteria such as IAE. The chaotic start-up enables the solution space to be explored more efficiently and serves to prevent local optima. On the whole, BCCFOA is better when it comes to the convergence speed and better control under dynamic charging conditions.

3.3.1. Initialization -Chaotic Sequence Generation

Each fish solution is initialized randomly in a binary form

$$X_i=\{x_{i1},x_{i2},..,x_{id}\}, \quad x_{ij}\in\{0,1\} \quad (7)$$

Where the fish’s position is X_i The number of decision variables is denoted by d. To enhance the randomness, the logistic map sequence is updated:

$$C_{t+1}=\mu C_t(1-C_t), \quad \mu\in(3.57, 4) \quad (8)$$

Where chaotic value at t iteration. This sequence helps escape local optima and improves exploration.

3.3.2. Fitness Evaluation

Each fish’s binary solution is decoded and evaluated using an objective function, such as:

$$f(X_i)=ITAE=\int_o^T t|e(t)|dt \quad (9)$$

Where e(t) is the control error for PID tuning, and the simulation time is represented as T.

3.3.3. Binary Conversion

Since the update may result in continuous values, a transfer function is used to convert binary form to an S-shaped transfer function.

$$S(x)=\frac{1}{1+e^{-x}} \quad (10)$$

The binary decision is

$$x_{i,j}^{t+1}=\begin{cases} 1, & \text{if } S\left(x_{ij}^{t+1}\right)>\text{rand}() \\ 0, & \text{otherwise} \end{cases} \quad (11)$$

3.3.4. Exploration Phase ($C_E/MaxC_E<0.5$)

BCCFOA resembles the early phase of fishing in which individual fishermen are scanning the waters in most directions. Fishermen go on their own and stir the water to bring the fish to the surface or to cause ripples. To investigate the global search space through diversity encouragement. The parameter α (capture rate), used in the algorithm, is calculated as:

$$\beta=\left(1-\frac{3\times C_E}{2\times MaxC_E}\right)^{\frac{3\times C_E}{2\times MaxC_E}} \quad (12)$$

The Catch Fish Optimization Algorithm assumes that in case the random number p is such that $p \geq 0.02$, then the agent uses the group-based capture behavior, in which they move in a common direction towards a common center.

When p< Beta, it does an independent search and looks at the space one at a time according to local feedback and random drift.

3.3.5. Independent Search (Exploration Formulae)

Fishermen disturb the water to float the fish, determine the position of the fish, and adjust the direction of exploration. The update formula is as follows:

$$Exp=\frac{fit_i-fit_p}{fit_{max}-fit_{min}} \quad (13)$$

Radius (R) of search based on progress

$$R=Dis\times\sqrt{|Exp|}\times\left(1-\frac{C_E}{MaxC_E}\right) \quad (14)$$

The position is updated by

$$Fisher_{i,j}^{T+1}=Fisher_{i,j}^{T}+\left(Fisher_{pos,j}^{T}-Fisher_{i,j}^{T}\right)\times Exp+r_s\times s\times R \quad (15)$$

In the above expressions, C, C E, and Max C E C E E Euclidean distance of reference and agent is denoted by Dis s and r s c are random unit vectors, and s c r c is an element in the zero to one range.

3.3.6. Exploitation Phase ($C_E/MaxC_E\geq 0.5$)

This step corresponds to the subsequent stage of the search, which is to refine the search around the best-known solution by means of cooperative behavior. Fishermen surround escaping fish with a Gaussian-based movement "σ" which allows a local exploitation that is focused around the global best.

$$\sigma=\sqrt{\frac{2\left(1-\frac{C_E}{MaxC_E}\right)}{\left(1-\frac{C_E}{MaxC_E}\right)^2+1}} \quad (16)$$

Towards the global best, the position is updated by

$$Fisher_i^{T+1}=G_{best}+GD\left(0,\frac{r_4\times\sigma\times|Mean\ (\mu)-G_{best}|}{3}\right) \quad (17)$$

Where G is the global optimum, 0 is the best, GD (0, s) is a Gaussian Distribution with mean 0 and variance s, and r 4 is a random number, and Mean (0 is the matrix of mean values per dimension of the center of the fishermen's location. Lastly, the solution is chosen depending on the minimization of the error criterion, and the PID controller is tuned to achieve the best results. The analysis of the BCCFOA pseudo code is presented in Table 2.

Table 2. Pseudo code for BCCFOA

Algorithm 1. Pseudo code for BCCFOA

Input: Population size N, Dimension d, Max evaluations MaxCE, Chaotic parameter μ
Initialize:
For i = 1 to N do
Randomly initialize binary position Xi of fish i
Initialize chaotic value Ci
Generate a logistic sequence for diversity
Evaluate the fitness of Xi using ITAE
End For
Set G_{best}= best solution based on fitness
Set C_E= 0 // Current evaluation count
 	
While $C_E/MaxC_E$<0.5 do
For i = 1 to N do
Calculate capture rate β
Generate a random number p in [0,1]
 	
If p < β then
// Exploration Phase: Independent Search
Select a random peer fish p ≠ i
Compute search direction and radius
Update position of fish i (continuous value)
Else
// Exploitation Phase: Group-Based Capture
Compute group center
Update the position of fish i toward the center using the Gaussian move
End If
Apply the transfer function to updated values
Convert to binary using the threshold rule
End For
 	
Evaluate the fitness of all fish.
Update Gbest if a new best is found
Increment CE
End While
Return Gbest as optimal PID parameters.

4. Results and Discussions

Figure 6 in the Simulink model represents a DAB DC-DC converter with a PID controller used in the charging of EV batteries. The DAB converter H-bridge topology is used in the model to ensure that power flows in both directions, which ensures proper energy transfer between the EV battery and the source. To ensure that desirable battery charging profiles, in either of the two modes, the PID controller is employed to ensure that the output voltage and current are controlled with precision. The model has different blocks that depict the voltage and current measurement circuit, feedback, choice of mode to be applied to the dynamic charging strategies, and SoC estimation. The model with the emphasis of blue is the battery model, where the electrochemical characteristics of the EV battery are modeled under varying charging conditions. The high-fidelity transient response analysis is with discrete simulation settings having a fine step size of "1x" 10 -7" seconds. This full Simulink system allows a complete assessment of the converter performance, and this confirms the usefulness of the PID controller in establishing a stable and efficient EV battery charging. Figure 7 of the input current waveform indicates that the converter has stabilized the dynamic current operating at an amplitude of 2 A after 0.7 s; at approximately 0.1 s, there is a sharp increase in amplitude of the input current, which reaches a peak of about 9.5 A before oscillating about this point, a result of dynamic current stabilization by the PID-controlled DAB converter. Conversely, the input voltage waveform of Figure 8 is barely out-of-band (within +0.5 V), and it is kept at a strict 300 V throughout the 1-second interval. This is to show the efficiency of the PID controller in making the voltage steady in its operation under transient and steady-state charging conditions to provide reliable and consistent energy transfer to the EV battery. The current waveform (Figure 9) has a slow increase up to approximately 2.7 A within 0.3 seconds, then shows some short oscillations, which, however, relax, and the steady-state current of approximately 2.65 A is achieved throughout the entire 1-second timeframe. This conduct is indicated in its output voltage waveform in Figure 10 that reaches an approximate of 270 V in the first quarter of a second, has a minute overshoot at approximately 275 V and then stabilizes at approximately 270 V. This demonstrates that the DAB converter under the control of PID has an outstanding regulation performance and satisfactory transient response, which ensures the battery receives a constant charging voltage and current that are required to charge the EV battery safely and efficiently.

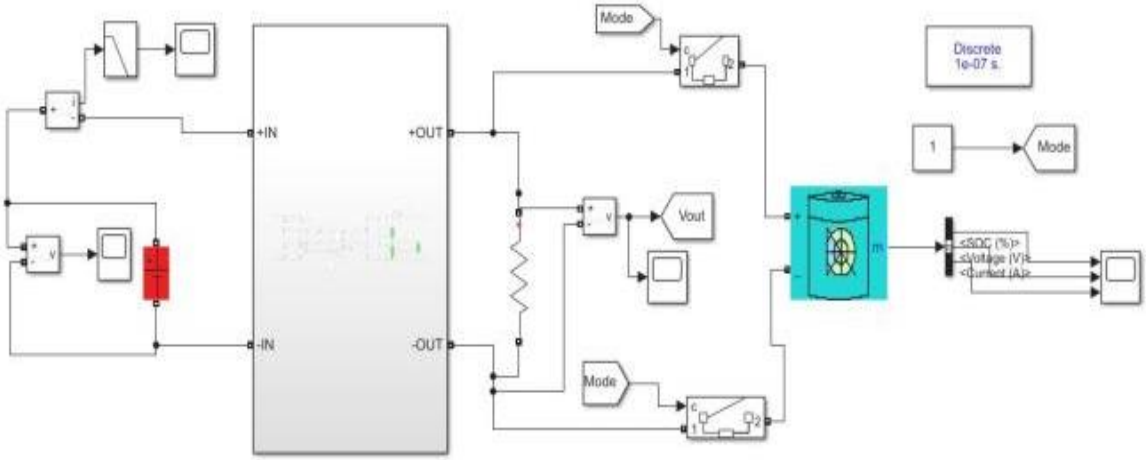

Fig. 6 Output voltage analysis

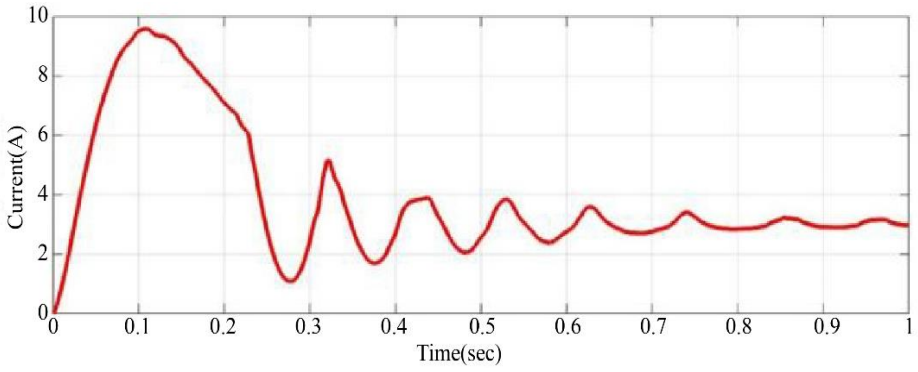

Fig. 7 Input current analysis

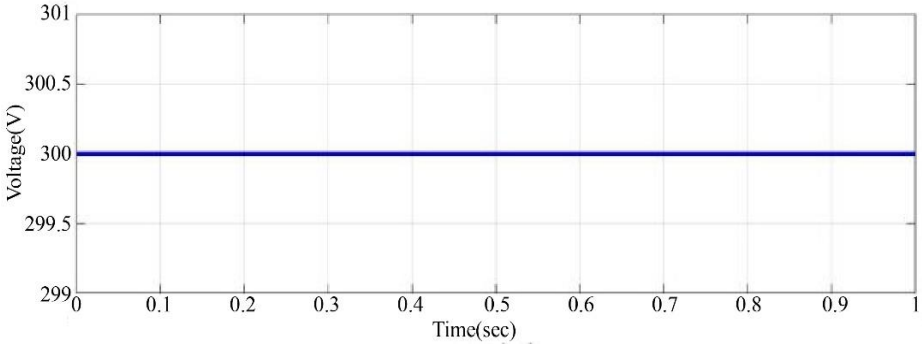

Fig. 8 Input voltage analysis

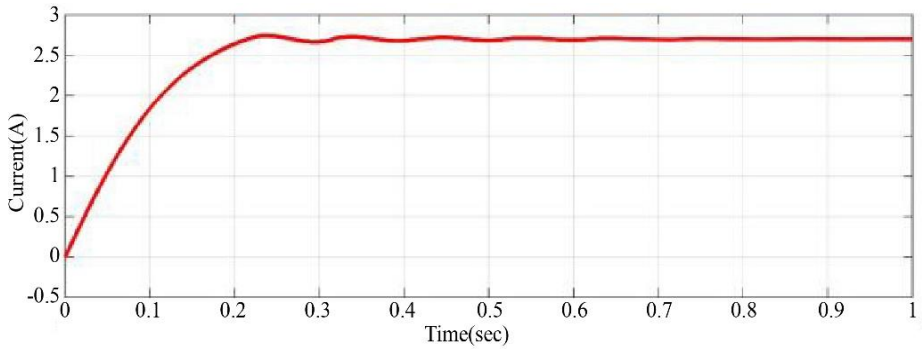

Fig. 9 Output current analysis

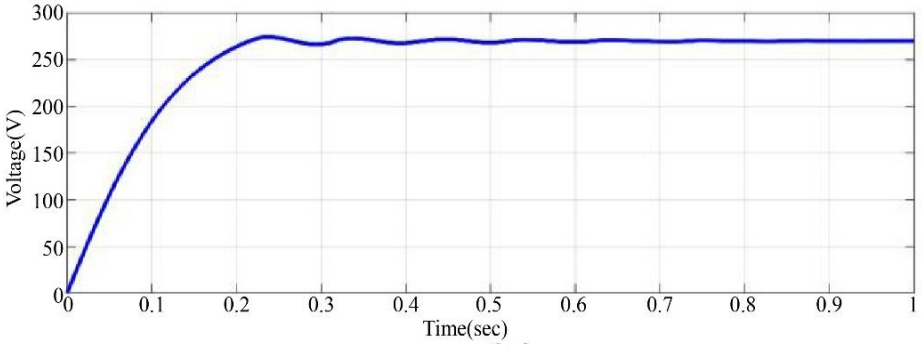

Fig. 10 Modeling of simulink

The battery voltage waveform Figure 11 indicates that there is a rise of 200 V that is instant and steady at the beginning of the simulation which remains at a fixed level during the duration of the simulation 1s.

This is a smooth, not fluctuating voltage profile, meaning that the DAB converter being controlled by PID successfully stabilizes the desired battery voltage, neither over nor undershooting or drifting, which is essential to come up with safe and reliable battery charging.

In the meantime, Figure 12 of battery current waveform indicates an initial sharp spike to about 2x -107 -4 already at time zero, with a rapid exponential decay, whose value levels off around zero but with small oscillations about the baseline. Accordingly, the State of Charge (SoC) curve Figure 13 originates at approximately 54.95%, and only slightly decreases up to 0.3 s, and then gradually rises to approximately 54.95% at 1 s. This small SoC increase is indicative of a regulated, small energy input into the battery, which is per the low charging current, indicative of accurate and predictable charging activity.

The convergence behavior of the fitness function, which is the ITAE when tuning PID controllers by BCCFOA, is provided in Figure 14 and compared with Catchfish Optimization Algorithm (CFOA), Tunicate Swarm Algorithm (TSA), and PSO. The ITAE measure punishes steady-state mistakes and, therefore, prefers quick and steady responses, which is why it is suitable to control systems that require fine-tuning. The y-axis of the graph is the fitness (ITAE value), whereas the x-axis is the number of iterations until 15. Reduced values of fitness show improved performance of the controller as time passes without much error.

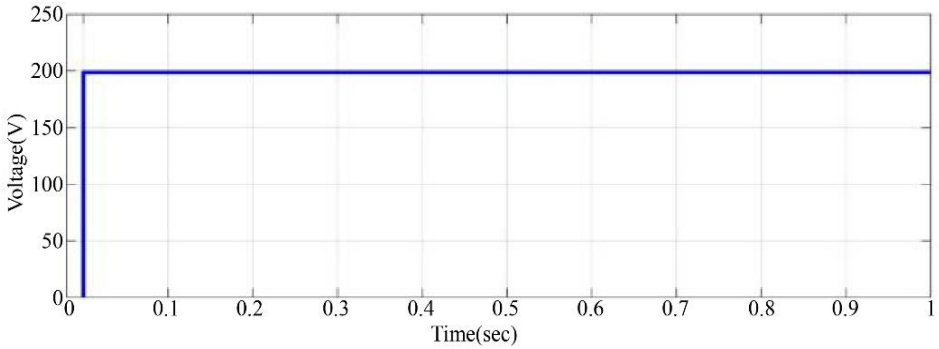

Fig. 11 Battery voltage analysis

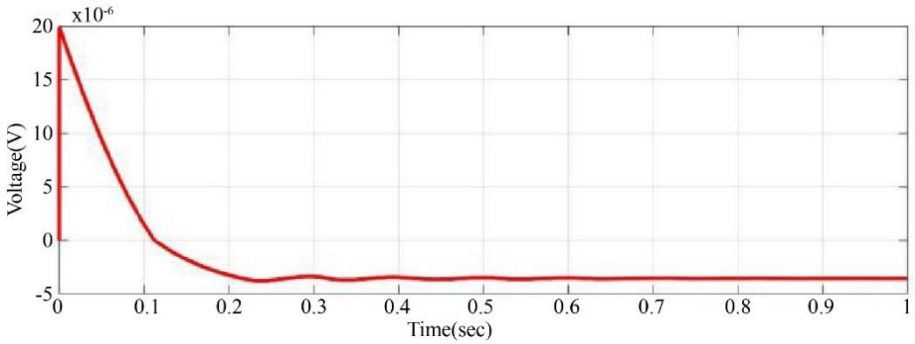

Fig. 12 Battery voltage analysis

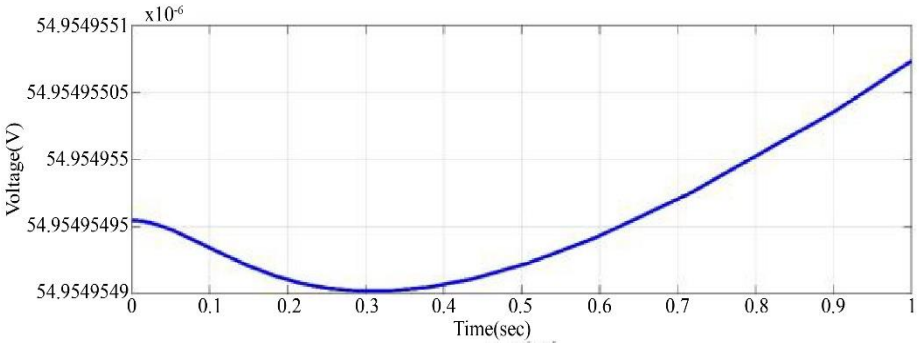

Fig. 13 Battery SOC state

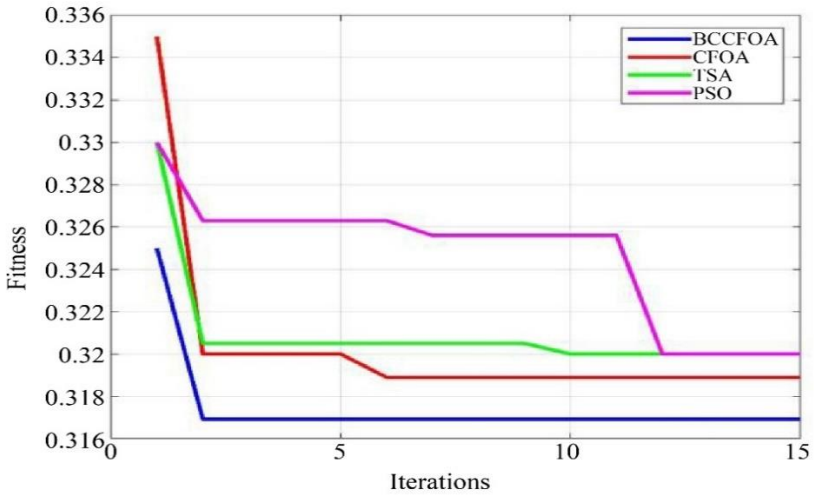

Fig. 14 Convergence curve comparative analysis

Proposed BCCFOA has the least final fitness value and converges fast within the initial few iterations, and ensures high levels of performance throughout, which elucidates its capacity to minimize the ITAE effectively. Conversely, CFOA, TSA, and PSO diverge at a slower rate and converge at higher fitness values, implying that they do not tune their PID parameters optimally. The high convergence of BCCFOA points out the benefits of combining binary encoding and chaotic maps to increase the exploration and prevent premature convergence, allowing the PID controller to obtain a shorter settling time, less overshoot, and better overall stability of the EV battery charging system.

Table 3. Fitness-based comparison

Algorithms	STD	K_P	K_I	K_D
BCCFOA (proposed)	2.084414e-03	4.113147e+02	3.734383e+02	3.087653e+02
CFOA	4.106035e-03	3.219157e+02	5.779221e+01	1.699595e+02
TSA	2.520393e-03	2.639340e+02	1.567874e+01	3.407577e+02
PSO	3.084910e-03	2.981712e+02	1.577060e+02	2.630318e+02

Table 3 shows the tuning results of the PID controller of four algorithms recommended by BCCFOA, CFOA, TSA, and PSO in terms of their attained Standard Deviation (STD) of the fitness (solution stability) and the optimization of the gains of the PID controller (K P I D). BCCFOA has the best STD of 2.08 x -1, 10 -1, which is highly stable and consistent in performance, and has much larger optimized gains (K P = 411.31, K I = 373.44, K D = 308.77), indicating a better responsive and better-tuned controller. Conversely, CFOA, TSA, and PSO have greater STDs and smaller balanced PID gains, which implies relatively poor convergence and ideal tuning. This underscores the efficiency of BCCFOA in developing accurate, stable, and strong optimization of PID parameters of the EV battery charging system.

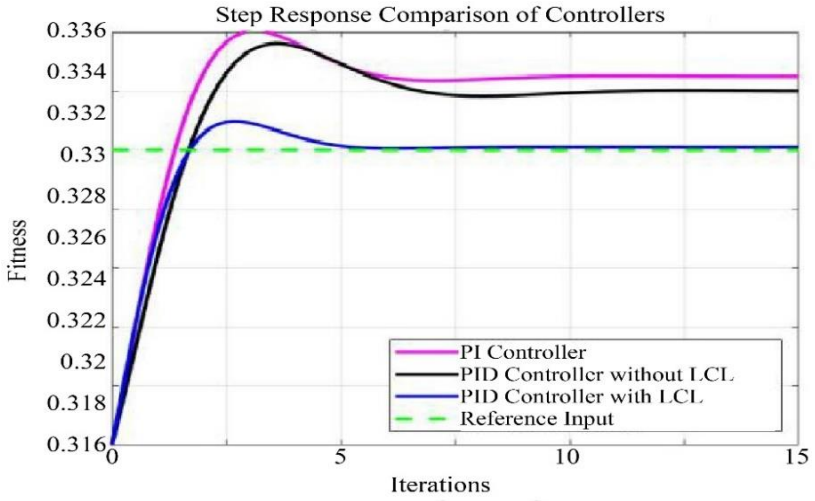

Fig. 15 Step response comparison

The comparison step response Figure 15 of the results indicates that the PI controller, the PID controller without LCL, and the PID controller with LCL have marked performance differences. The PI controller has the worst overshoot of about 37 percent of the total, with the output value of about 1.37, then stabilizing.

It also has a rising time of about 0.38 seconds and a settling time of nearly 2.2 seconds, indicating that it takes longer to stabilize. The PID controller without LCL has a better response (with an overshoot of approximately 29 percent), settles in approximately 1.7 seconds, and has a rising time of approximately 0.35 seconds. Having a small peak overshoot of approximately 5%, a short settling time of 1.0 seconds, and the highest rise time of approximately 0.28 seconds, the PID controller with LCL works better. Based on these results, the LCL filter is significantly better than the conventional one in terms of transient response, precision, and overall system stability.

5. Conclusion

An intelligent DAB-based EV-charging framework based on improved power quality and optimal control has been constructed and tested. The system is without doubt helpful in dual-mode charging using DPS to operate at Constant Voltage and EPS to operate at Constant Current. Compared to CFOA, TSA, and PSO, the PID controller, which is tuned with the BCCFOA algorithm with ITAE as the fitness function, has better convergence and performance. The BCCFOA- tuned PID controller had a remarkably high fitness standard

deviation of 2.0810-3, which indicated that the tuning consistency of the PID controller was good. The use of an LCL filter results in significantly improved transient response, and peak overshoot is reduced to 5%, settling time is reduced to 1.0 s, and rising time is also reduced to 0.28 s. Also, the SoC curve of the battery presents a steady and gradual charge pattern, with an increase to 54.95%. These results are testaments to the ability of the proposed system to offer high-quality power and fast, consistent, and efficient EV battery recharging. In order to evaluate the controller performance in realistic operating environments, the future study will focus on the application of Hardware-In-The-Loop (HIL) testing and real-time digital simulation on dSPACE platforms. Moreover, to perform real-time modulation, the predictive control methods based on adaptive control and artificial intelligence, such as Model Predictive Control (MPC) and reinforcement learning, will be explored. To promote scalability and intelligence of the proposed EV charging architecture under the smart grid setup, the renewable energy connection, grid-tied synchronization, and bidirectional V2G connectivity to the state-of-the-art cybersecurity solutions will also be considered.

References

[1] Alex V. Mirtchev, and Emmanuel C. Tatakis, "Design Methodology based on Dual Control of a Resonant Dual Active Bridge Converter for Electric Vehicle Battery Charging," *IEEE Transactions on Vehicular Technology*, vol. 71, no. 3, pp. 2691-2705, 2022. [CrossRef] [Google Scholar] [Publisher Link]

[2] Md Ahsanul Hoque Rafi, and Jennifer Bauman, "Optimal Control of Semi-Dual Active Bridge DC/DC Converter with Wide Voltage Gain in a Fast-Charging Station with Battery Energy Storage," *IEEE Transactions on Transportation Electrification*, vol. 8, no. 3, pp. 3164-3176, 2022. [CrossRef] [Google Scholar] [Publisher Link]

[3] Yousef Nazih et al., "A Ring-Connected Dual Active Bridge based DC-DC Multiport Converter for EV Fast-Charging Stations," *IEEE Access*, vol. 10, pp. 52052-52066, 2022. [CrossRef] [Google Scholar] [Publisher Link]

[4] Li Jiang et al., "Integrated Optimization of Dual-Active-Bridge DC-DC Converter with ZVS for Battery Charging Applications," *IEEE Journal of Emerging and Selected Topics in Power Electronics*, vol. 11, no. 1, pp. 288-300, 2023. [CrossRef] [Google Scholar] [Publisher Link]

[5] Deliang Chen et al., "A Dual-Transformer-based Hybrid Dual Active Bridge Converter for Plug-in Electric Vehicle Charging to Cope with Wide Load Voltages," *IEEE Transactions on Industrial Electronics*, vol. 70, no. 2, pp. 1444-1454, 2023. [CrossRef] [Google Scholar] [Publisher Link]

[6] Marzio Barresi, Edoardo Ferri, and Luigi Piegari, "An MV-Connected Ultra-Fast Charging Station based on MMC and Dual Active Bridge with Multiple Dc Buses," *Energies*, vol. 16, no. 9, pp. 1-23, 2023. [CrossRef] [Google Scholar] [Publisher Link]

[7] Sara J. Ríos, Daniel J. Pagano, and Kevin E. Lucas, "Bidirectional Power Sharing for DC Microgrid Enabled by Dual Active Bridge DC-DC Converter," *Energies*, vol. 14, no. 2, pp. 1-24, 2021. [CrossRef] [Google Scholar] [Publisher Link]

[8] Liting Li et al., "Review of Dual-Active-Bridge Converters with Topological Modifications," *IEEE Transactions on Power Electronics*, vol. 38, no. 7, pp. 9046-9076, 2023. [CrossRef] [Google Scholar] [Publisher Link]

[9] Ganesh Chilakalapudi, and Amritesh Kumar, "Optimal Reactive Power Control for Dual-Active-Bridge Converter using Improved Dual-Phase-Shift Modulation Strategy for Electric Vehicle Application," *International Journal of Circuit Theory and Applications*, vol. 51, no. 3, pp. 1204-1223, 2023. [CrossRef] [Google Scholar] [Publisher Link]

[10] Song Hu et al., "Sinusoidal-Ripple-Current Charging Modulation for Semi-Dual-Active-Bridge AC-DC Converter with Full Soft Switching and Power Factor Correction," *IEEE Transactions on Circuits and Systems II: Express Briefs*, vol. 71, no. 1, pp. 326-330, 2024. [CrossRef] [Google Scholar] [Publisher Link]

[11] Balakrishna Nallamothu, B. Santhana Krishnan, and Ravindra Janga, "Comprehensive Analysis of PI and Fuzzy-Controlled Dual Active Bridge Converter for Renewable Energy-based Off-Board EV Charging," *International Journal of Multiphysics*, vol. 18, no. 3, pp. 1178-1190, 2024. [Google Scholar] [Publisher Link]

[12] Khurshid Ul Haq, Farhad Ilahi Bakhsh, and Obbu Chandra Sekhar, "Improved Performance of Dual Active Bridge Converter using Particle Swarm Optimization based Phase Shift Modulation for EV Application," *Distributed Generation and Alternative Energy Journal*, vol. 40, no. 2, pp. 361-400, 2025. [CrossRef] [Google Scholar] [Publisher Link]

[13] Felipe Ruiz et al., "A High-Performance Fractional Order Controller based on Chaotic Manta-Ray Foraging and Artificial Ecosystem-based Optimization Algorithms Applied to Dual Active Bridge Converter," *Fractal and Fractional*, vol. 8, no. 6, pp. 1-19, 2024. [CrossRef] [Google Scholar] [Publisher Link]

[14] Zhangyong Chen et al., "Efficiency Improvement of Dual Active Bridge Converter using Simple Graphical Optimization Method," *International Journal of Circuit Theory and Applications*, vol. 52, no. 1, pp. 248-262, 2024. [CrossRef] [Google Scholar] [Publisher Link]

[15] Dabin Jia, and Dazhi Wang, "Current Stress Minimization based on Particle Swarm Optimization for Dual Active Bridge DC-DC Converter," *Actuators*, vol. 13, no. 10, pp. 1-18, 2024. [CrossRef] [Google Scholar] [Publisher Link]

[16] Izza Anshory et al., "Optimization DC-DC Boost Converter of BLDC Motor Drive by Solar Panel using PID and Firefly Algorithm," *Results in Engineering*, vol. 21, pp. 1-10, 2024. [CrossRef] [Google Scholar] [Publisher Link]

[17] Mostafa Jabari et al., "Performance Analysis of DC-DC Buck Converter with Innovative Multi-Stage PIDn (1+ PD) Controller using GEO Algorithm," *Scientific Reports*, vol. 14, no. 1, pp. 1-21, 2024. [CrossRef] [Google Scholar] [Publisher Link]

[18] Ashish Choubey, Sachin Kumar Jain, and Prabin Kumar Padhy, "A GWO-Optimized FSIMC-PID Controller for Sustained Operation of DC-DC Boost Converter," *2024 1st International Conference on Sustainability and Technological Advancements in Engineering Domain (SUSTAINED)*, Faridabad, India, pp. 23-27, 2024. [CrossRef] [Google Scholar] [Publisher Link]

[19] Mostafa Jabari, and Amin Rad, "Optimization of Speed Control and Reduction of Torque Ripple in Switched Reluctance Motors using Metaheuristic Algorithms based PID and FOPID Controllers at the Edge," *Tsinghua Science and Technology*, vol. 30, no. 4, pp. 1526-1538, 2025. [CrossRef] [Google Scholar] [Publisher Link]

[20] Mohamed A.M. Shaheen et al., "Walrus Optimizer-based Optimal Fractional Order PID Control for Performance Enhancement of Offshore Wind Farms," *Scientific Reports*, vol. 14, no. 1, pp. 1-17, 2024. [CrossRef] [Google Scholar] [Publisher Link]

[21] Mridul Mishra, and Indrajit Sarkar, "EV Battery Charging using DAB DC-Dc Converter with EPS and DPS Modulations," *IEEE International Students' Conference on Electrical, Electronics and Computer Science (SCEECS)*, Bhopal, India, pp. 1-6, 2023. [CrossRef] [Google Scholar] [Publisher Link]

[22] Heming Jia et al., "Catch Fish Optimization Algorithm: A New Human Behavior Algorithm for Solving Clustering Problems," *Cluster Computing*, vol. 27, no. 9, pp. 13295-13332, 2024. [CrossRef] [Google Scholar] [Publisher Link]